OxLDL increases endothelial stiffness, force generation, and network formation[S]

Fitzroy J. Byfield,* Saloni Tikku,* George H. Rothblat,† Keith J. Gooch,* and Irena Levitan[1,*]

Institute for Medicine and Engineering,* Department of Pathology and Laboratory Medicine, University of Pennsylvania, Philadelphia, PA 19104; and Department of Pediatrics,† Children's Hospital of Philadelphia, Philadelphia, PA 19104

Abstract **This study investigates the effect of oxidatively modified low density lipoprotein (OxLDL) on the biomechanical properties of human aortic endothelial cells (HAECs). We show that treatment with OxLDL results in a 90% decrease in the membrane deformability of HAECs, as determined by micropipette aspiration. Furthermore, aortic endothelial cells freshly isolated from hypercholesterolemic pigs were significantly stiffer than cells isolated from healthy animals. Interestingly, OxLDL had no effect on membrane cholesterol of HAECs but caused the disappearance of a lipid raft marker, GM_1, from the plasma membrane. Both an increase in membrane stiffness and a disappearance of GM_1 were also observed in cells that were cholesterol-depleted by methyl-β-cyclodextrin. Additionally, OxLDL treatment of HAECs embedded within collagen gels resulted in increased gel contraction, indicating an increase in force generation by the cells. This increase in force generation correlated with an increased ability of HAECs to elongate and form networks in a three-dimensional environment. Increased force generation, elongation, and network formation were also observed in cholesterol-depleted cells. We suggest, therefore, that exposure to OxLDL results in the disruption or redistribution of lipid rafts, which in turn induces stiffening of the endothelium, an increase in endothelial force generation, and the potential for network formation.**—Byfield, F. J., S. Tikku, G. H. Rothblat, K. J. Gooch, and I. Levitan. **OxLDL increases endothelial stiffness, force generation, and network formation.** ***J. Lipid Res.*** **2006.** 47: **715–723.**

Supplementary key words endothelial cells • cholesterol • cell stiffness • endothelial morphogenesis

Oxidative damage of LDL is associated with an increased risk for coronary artery disease and plaque formation (1–3). Earlier studies have demonstrated that oxidized low density lipoprotein (OxLDL) is present in atherosclerotic lesions in human and rabbit arteries (3) and that the level of OxLDL increases dramatically with hypercholesterolemia both in animal models, such as miniature pigs (4) and monkeys (5), and in humans (6, 7). It is also well known that exposure to OxLDL results in endothelial dysfunction, including disruption of the endothelial barrier (8), impairment of nitric oxide release (9), and endothelial cell (EC) migration (10, 11). In this study, we focus on the role of OxLDL in the regulation of endothelial biomechanical properties, which play a major role in multiple EC functions, such as endothelial network formation, wound repair, and mechanotransduction.

Recent studies have shown that exposure of ECs to OxLDL, rather than enriching the cells with cholesterol, removes cholesterol from cholesterol-rich membrane domains (lipid rafts) and induces the internalization of these domains (9, 12). One of the important remaining questions is how OxLDL-induced changes in endothelial cholesterol affect the biomechanical properties of these cells. Our recent studies have shown that, in contrast to artificial lipid bilayers, in which removal of cholesterol decreases the stiffness of membrane lipid bilayers (13), ECs become stiffer upon cholesterol depletion (14, 15). Because it is known that cellular stiffness/deformability depends strongly on the submembrane cytoskeleton (16, 17), an increase in cellular stiffness suggests that cholesterol removal alters the biomechanical properties of the membrane-cytoskeleton complex and makes it stiffer.

Importantly, recent studies have indicated that increased cellular stiffness is correlated with the magnitude of forces that cells exert on substrates (18). Cell-derived forces in turn result in matrix compaction and remodeling (19). Furthermore, it was shown that across different human EC lines (large vessel, microvascular, and blood-derived), force generation correlated with the extent to which the cells formed three-dimensional networks in collagen gels (20, 21), an established in vitro model of EC morphogenesis. Many in vivo processes can be recapitulated in this system, including endothelial cell elongation, lumen formation, and cell-cell interactions, all suggestive

Manuscript received 5 October 2005 and in revised form 27 December 2005.

Published, JLR Papers in Press, January 17, 2006.
DOI 10.1194/jlr.M500439-JLR200

[1] To whom correspondence should be addressed.
e-mail: ilevitan@mail.med.upenn.edu

[S] The online version of this article (available at http://www.jlr.org) contains two additional figures.

of increased angiogenic potential. This system has been used to investigate multiple endothelial functions, including the mechanisms of action of angiogenic growth factors and angiogenesis inhibitors (22, 23). Our study shows that exposure to OxLDL increases both the stiffness and the forces exerted by the cells on the substrate and facilitates EC network formation.

METHODS

Cells

Human aortic endothelial cells (HAECs; BioWhittaker, Rutherford, NJ) were maintained between passages three and five in 2% fetal bovine serum endothelium growth medium-2 (EGM-2; Cambrex), as described previously (24).

Pig aortic endothelial cells (PAECs) were isolated from aortas of normal and hypercholesterolemic Yorkshire pigs. Briefly, the pigs were fed either standard low-cholesterol chow (control group) or high-cholesterol chow supplemented with 10% lard and 0.5% cholesterol for 3–6 months. The high-cholesterol diet resulted in a significant increase in the level of plasma cholesterol (~300 mg/dl), whereas in control pigs cholesterol remained at <100 mg/dl. PAECs were isolated by gentle mechanical scraping on the inner surface of aortas immediately after sacrifice, as described previously (25). The purity of endothelial cells was verified by staining the cells with two endothelial markers: platelet endothelial cell adhesion molecule (PECAM) and von Willebrand factor (>95% of cells were positive for both markers and negative for smooth muscle actin). The protocol was approved by the Institutional Animal Care and Use Committee of the University of Pennsylvania. The University of Pennsylvania is Association for Assessment of Laboratory Animal Care (AALAC)-accredited.

Cholesterol reagents

LDL and OxLDL (Biomedical Technologies, Stoughton, MA) were dissolved in EGM-2 supplemented with 0.2% FBS to a final concentration of 10–50 μg/ml. Thiobarbituric acid-reactive (TBAR) substances were assayed as a measure of oxidative lipid modification. Methyl-β-cyclodextrin (MβCD; Sigma Chemical, St. Louis, MO) was also dissolved in 0.2% or serum-free EGM-2.

Micropipette aspiration

Micropipette aspiration of substrate-attached endothelial cells was performed as described in our earlier study (15). Briefly, the membranes were visualized with a fluorescent membrane dye, carbocyanide $DiIC_{18}$ (Molecular Probes, Eugene, OR), and then aspirated using micropipettes with 3–5 μm outer diameter pulled from borosilicate glass capillaries (SG10 glass; Richland Glass, Richland, NJ). Negative pressure was applied to a pipette by a pneumatic transducer tester (BioTek Instruments, Winooski, VT).

Cholesterol measurement and cholera toxin staining

Cholesterol was measured with the Amplex Red cholesterol assay kit (Molecular Probes) according to the manufacturer's specifications. EC membrane fractions were isolated using a detergent-free method, as described (26). Localization of GM_1 was determined by incubating HAECs with Alexa 488-conjugated cholera toxin (Molecular Probes) at a concentration of 50 μg/ml in 0.1% BSA for 40 min on ice. Cells were then washed, mounted, and viewed using a Zeiss Axiovert 100TV microscope (Zeiss, Jena, Germany). For analysis, 20 images were taken per experimental condition, and the average fluorescence intensity was determined using Meta-View software.

Preparation of gels and visualization of embedded endothelial cells

Collagen gels were prepared according to the manufacturer's instructions to a final collagen concentration of 1.5 mg/ml (Becton Dickinson, Franklin Lanes, NJ). HAECs were seeded into gel mixtures at 1×10^6/ml, and gels were allowed to polymerize for 45 min at 37°C in well plates. Thereafter, the gels were mechanically loosened from the sides of the wells, and growth medium supplemented with vascular endothelial growth factor, basic fibroblast growth factor (R&D Systems, Minneapolis, MN), and phorbol myristate acetate (Sigma Chemical) at concentrations of 50 μg/ml each was added. Gels were cultured for 48 h and imaged with a Nikon Coolpix 4500 digital camera, and gel contraction was quantified using Scion Image (Las Vegas, NV).

To visualize the cells, gels were fixed in 4% paraformaldehyde for 40 min, stained for 5 min in 0.1% toluidine blue, which stains cells darkly and extracellular matrix faintly, or treated for 40 min in 1 μM rhodamine-phalloidin (Molecular Probes). Images of toluidine blue staining were obtained at 10× magnification to observe EC networks, whereas actin images were obtained at 63× magnification to observe cell-cell connections (Zeiss Axiophot microscope; Zeiss, Thornwood, NY). For network quantification, five images were taken per gel from three gels per experimental condition, threshholded, made binary, and skeletonized using built-in Scion Image functions as described previously (20). For lumen visualization, gels were fixed, dehydrated, embedded in paraffin, sectioned, and stained with Masson's trichrome blue (Richard-Allen Scientific, Kalamazoo, MI). Lumens were defined as collagen-free areas surrounded by cellular bodies. Ten micrometer sections were cut from each gel, and 15 images containing one or more lumens were taken per experimental condition using 10× magnification.

RESULTS

OxLDL increases cellular stiffness of HAECs

HAECs were exposed to 10–50 μg/ml OxLDL, levels similar to the circulating levels of OxLDL in human plasma (7–35 μg/ml) (27). Similar to earlier studies (9, 11), the oxidation state of LDL was 10–15 nmol/mg protein TBAR, consistent with the LDL oxidation level reported for atherosclerotic lesions (11 nmol/mg protein TBAR) (3). Two types of controls were used in this study: exposure to the same levels of nonoxidized LDL, and exposure to the growing medium alone. Representative images and the time courses of membrane deformation show that membrane projections in OxLDL-treated cells were significantly shorter than in cells treated with nonoxidized LDL or in cells that were exposed to medium alone, indicating that OxLDL-treated cells were less deformable than the other two experimental cell populations (**Fig. 1**). Membrane deformation was analyzed at 2–5 mm Hg negative pressure because in HAECs, membrane projections typically started to develop at −2 mm Hg and could be maintained at −5 mm Hg, whereas higher pressures resulted in breakage of the membrane. Significant differences between the lengths of membrane projec-

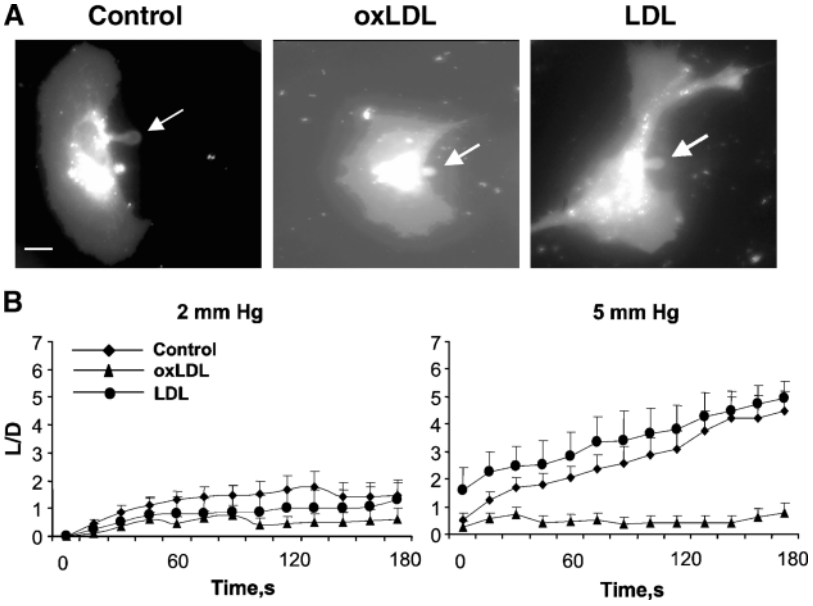

Fig. 1. Oxidized low density lipoprotein (OxLDL), but not LDL, constrains membrane deformation of human aortic endothelial cells (HAECs). A: Typical images of membrane deformation for cells treated with 10 μg/ml OxLDL or 10 μg/ml LDL for 1 h compared with low-serum control. The images show the maximal deformation at −5 mm Hg. Arrows indicate the positions of the aspirated projections. Bar = 30 μm. B: Average time courses of aspirated lengths of OxLDL- and LDL-treated cells and of nontreated controls at −2 and −5 mm Hg. The graphs show means + SEM (n = 19, 14, and 7 for control, OxLDL, and LDL respectively). The difference between control and OxLDL is statistically significant ($P < 0.05$).

tions were observed at both pressures. Noteworthy, the stiffening was observed after 1 h of OxLDL exposure, and no further effect developed after prolonging the exposure to 6 h (**Fig. 2**). No difference was observed between 10 and 50 μg/ml OxLDL (data not shown).

Plasma hypercholesterolemia increases EC stiffness in vivo

There is a general consensus that OxLDL is one of the major factors in hypercholesterolemia-induced cellular dysfunction and that the levels of OxLDL increase in hypercholesterolemic plasma. Specifically, strong increases in OxLDL were reported in plaques of diet-induced atherosclerotic miniature pigs (high-cholesterol diet for 3–6 months) (4) and hypercholesterolemic rabbits (3) as well as in plasma of hypercholesterolemic monkeys maintained on a high-cholesterol diet for 32 months (5). Therefore, we compared the stiffness of endothelial cells freshly isolated from the aortas of control and hypercholesterolemic pigs within 24 h after isolation. Representative images and time courses of membrane deformation of cells isolated from normal and hypercholesterolemic pigs are shown in **Fig. 3**. Cells appear rounded as they were aspirated within 24 h of isolation. In general, PAECs were stiffer than HAECs, so that the membrane could be deformed by applying at least −10 mm Hg, but the effect of plasma hypercholesterolemia on cell stiffness was similar to that of OxLDL. An increase in endothelial stiffness in

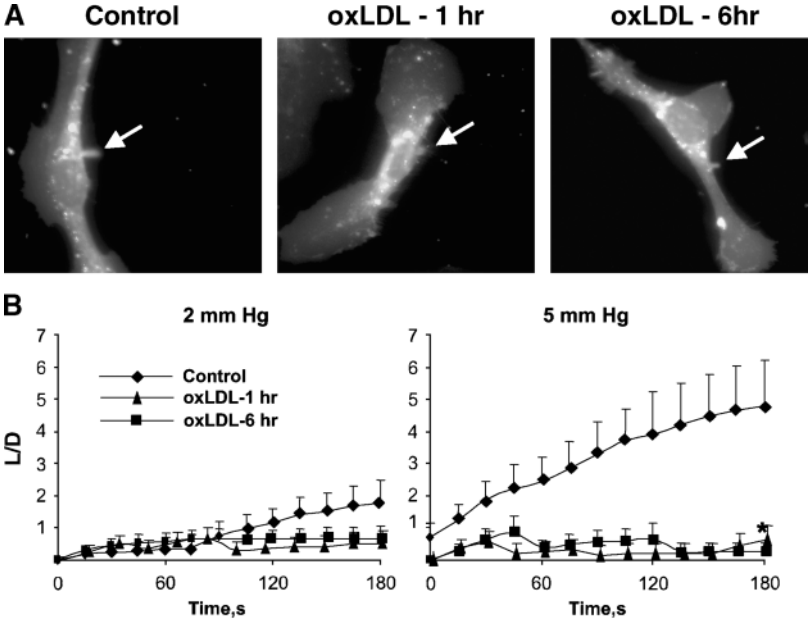

Fig. 2. Prolonged exposure to OxLDL has no further effect on membrane deformation. A: Representative images of membrane deformation for control cells and cells treated with OxLDL for 1 and 6 h. Images show the maximal deformation at −5 mm Hg. Arrows indicate the positions of the aspirated projections. Bar = 30 μm. B: Average time courses of aspirated lengths for control and OxLDL-treated cells at −2 and −5 mm Hg. The graphs show means + SEM (n = 7, 14, and 6 for control, 1 h, and 6 h).

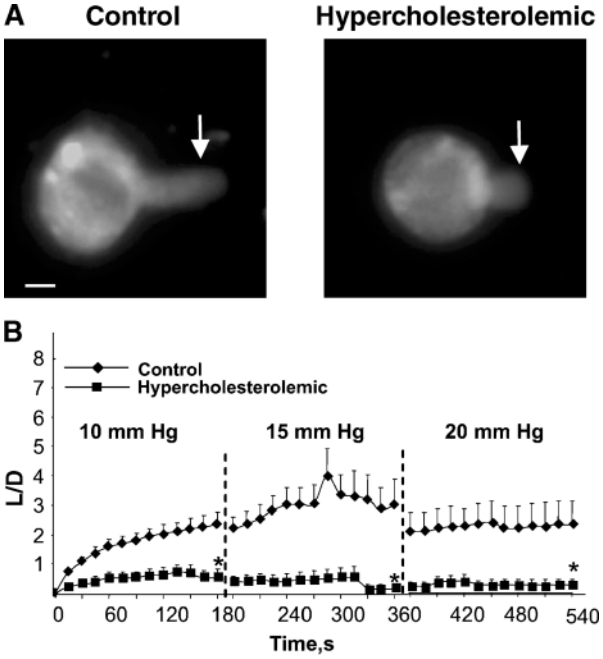

Fig. 3. Plasma hypercholesterolemia constrains membrane deformation in pig aortic endothelial cells (PAECs). A: Membrane deformation of PAECs at −15 mm Hg. Arrows indicate the position of the aspirated projections. Bar = 40 μm. B: Average time course of aspirated lengths for control cells and hypercholesterolemic cells at −10, −15, and −20 mm Hg. The graphs show means + SEM. Control, n = 35 cells; hypercholesterolemic, n = 40 cells. The difference between control and hypercholesterolemic conditions is statistically significant ($P < 0.05$).

cells freshly isolated from hypercholesterolemic pigs indicates that hypercholesterolemia induces the stiffening of endothelial cells in vivo.

OxLDL-induced stiffening of HAECs can be simulated by cholesterol depletion

To test further the mechanism of OxLDL-induced endothelial stiffening, we investigated the relationship between OxLDL-induced stiffening and the level of cellular cholesterol. We have shown previously that endothelial stiffening is observed in bovine aortic endothelium when the cells are depleted of cholesterol but not when the cells are cholesterol-enriched (15). Furthermore, it was shown that exposure to OxLDL in vitro and hypercholesterolemia in vivo result in depleting cholesterol from endothelial caveolae (9, 28). We hypothesized, therefore, that OxLDL may increase endothelial stiffness by depleting endothelial cholesterol. To address this hypothesis, we tested *1*) whether OxLDL results in cholesterol depletion and/or redistribution of lipid rafts in HAECs, and *2*) whether the effect of OxLDL on HAEC stiffness can be simulated by cholesterol depletion.

To determine the effect of OxLDL on the level of membrane cholesterol in raft and nonraft membrane domains, membrane fractions were prepared using a nondetergent separation method based on the differential buoyancy of cholesterol-rich and cholesterol-poor membrane domains. As expected, membrane cholesterol shows a clear double peak distribution between the fractions, with the major peak in high-buoyancy fractions (lipid rafts) and a minor peak in low-buoyancy fractions (nonraft). Indeed, also as expected, the high-buoyancy fractions were enriched in caveolin (data not shown). Exposure of HAECs to OxLDL, however, had no effect on the level of membrane cholesterol either in raft or nonraft membrane fractions (**Fig. 4A**). The same results were obtained in four independent experiments. Importantly, exposure to OxLDL resulted in a decrease of surface expression of GM_1 (Fig. 4B), a major lipid raft marker (29), suggesting that OxLDL induces the internalization of caveolae/lipid rafts. Depleting cholesterol with MβCD resulted in a similar effect on GM_1. This is consistent with earlier studies demonstrating the internalization of caveolae/lipid rafts in OxLDL (9, 12) and in MβCD-treated cells (30).

To address the second question, the level of cellular cholesterol in HAECs was either chronically depleted by serum starvation for 24 h or acutely depleted by exposure to MβCD, resulting in an ∼40% or 80% decrease in cholesterol, respectively (**Fig. 5**, top). A decrease in cellular cholesterol resulted in a proportional increase in cell stiffness, as demonstrated by the representative images of control, serum-starved, and MβCD-treated cells (Fig. 5A) and by the average time courses of membrane deformation of the same three cell populations (Fig. 5B). In this series of experiments, cell stiffness was compared only at −5 mm Hg, because no aspiration was observed in MβCD-treated cells at lower pressures. Thus, our results show that although OxLDL had no significant effect on cholesterol levels of both raft and nonraft membrane fractions, its effect on HAEC stiffness could be simulated by both chronic and acute cholesterol depletion. Furthermore, when the cells were simultaneously exposed to OxLDL and depleted of cholesterol (by 24 h serum starvation), no additional stiffening was observed (data not shown), suggesting that OxLDL and cholesterol depletion affect endothelial stiffness through a common pathway.

OxLDL and cholesterol depletion increase force generation

The correlation between HAECs' stiffness and their ability to generate force on the cell-substrate interface was tested by measuring gel contraction by HAECs, as described previously (19, 20). As expected, seeding the cells into gels resulted in gel contraction under all experimental conditions (**Fig. 6A**; compare the gel that contains no cells with the rest of the gels). Importantly, however, cells that were pretreated with OxLDL or MβCD showed significantly greater gel contraction, as indicated by a decrease in gel area (Fig. 6A, B). As the same number of cells were seeded into each gel, these observations suggest that the contractile forces that OxLDL-treated and MβCD-treated cells applied to their substrates were stronger than the forces applied by control cells.

OxLDL and MβCD facilitate the formation of an EC network

Similar to other types of endothelial cells, HAECs embedded in collagen gels form lumens clear of collagen

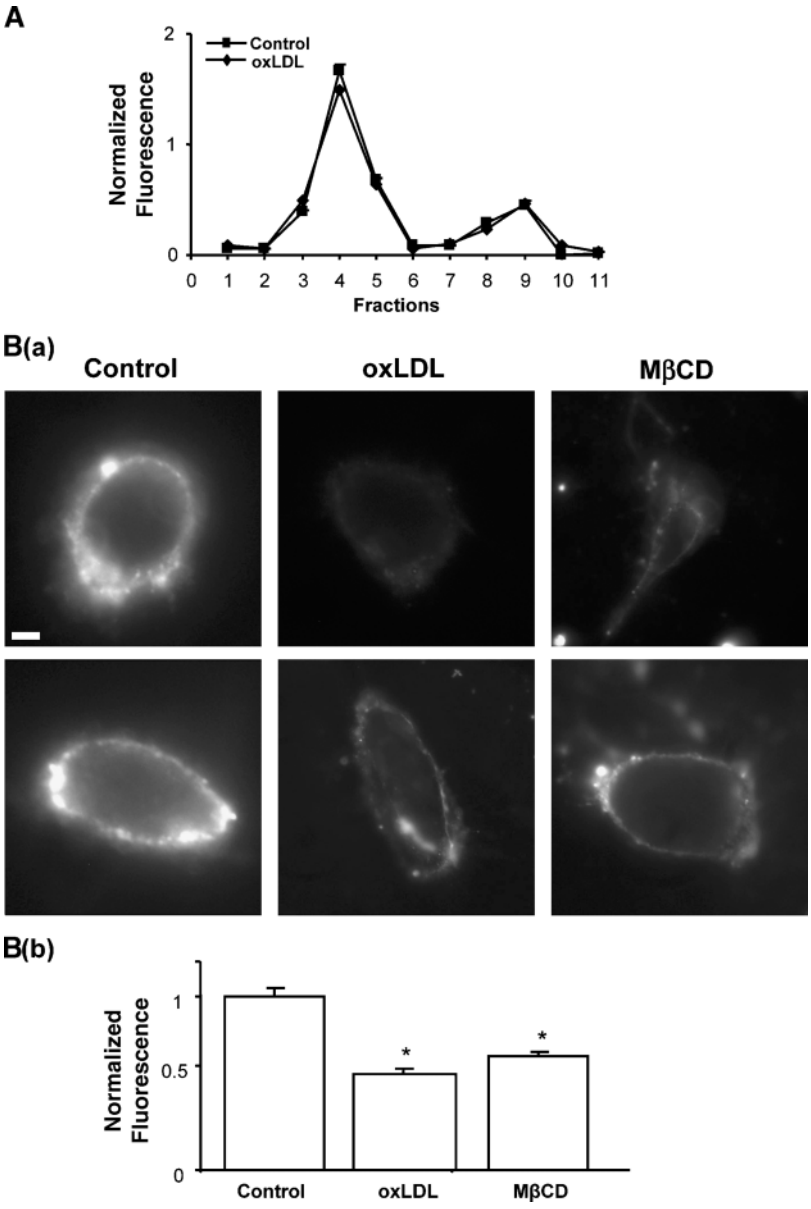

Fig. 4. Effect of OxLDL on cholesterol content and GM_1 distribution in HAECs. A: Cholesterol content in membrane fractions of HAECs. Ba: Typical images of fluorescently labeled cholera toxin (CTx) staining in nonpermeabilized control, OxLDL-treated, and methyl-β-cyclodextrin (MβCD)-treated cells showing localization of GM_1 in the membrane. Bb: Average intensity for each condition (20 cells per condition). Similar results were obtained in three independent ex periments. The graphs show means + SEM. * $P < 0.05$.

after 48 h in culture. Furthermore, cells treated with OxLDL or MβCD formed slightly larger lumens than those formed in control cells (see supplementary Fig. I). Visualizing the organization of the HAEC actin cytoskeleton demonstrates further that the cells form multiple connections within a gel under all three conditions (see supplementary Fig. II). Most importantly, although no significant difference was observed in the number of lumens under the three experimental conditions (see supplementary Fig. I), the degree of cell connectivity and elongation was significantly enhanced by OxLDL and MβCD. The difference between control and OxLDL or MβCD conditions is apparent from the images of the EC networks within the gels (**Fig. 7A**): whereas there are relatively few connecting cells in control gels, there are multiple connections in both OxLDL- and MβCD-treated cells. It is also apparent that the cells are more elongated under these conditions. To quantify these effects, the images were skeletonized, as recently described (20). The more elongated the cells are and the more connections they form, the longer are the uninterrupted lines in the skeletonized images. Therefore, the average length of the skeletonized image, a measure of the length of uninterrupted lines, was suggested to be an index of network formation. Our observations show that exposing HAECs to OxLDL or to MβCD resulted in doubling of the average length of skeletonization index, suggesting that OxLDL and cholesterol depletion have similar facilitatory effects on the ability of HAECs to form endothelial networks.

DISCUSSION

The goal of this study was to investigate the effects of OxLDL on biomechanical properties of vascular tissues at the cellular level. The main findings of this study are as

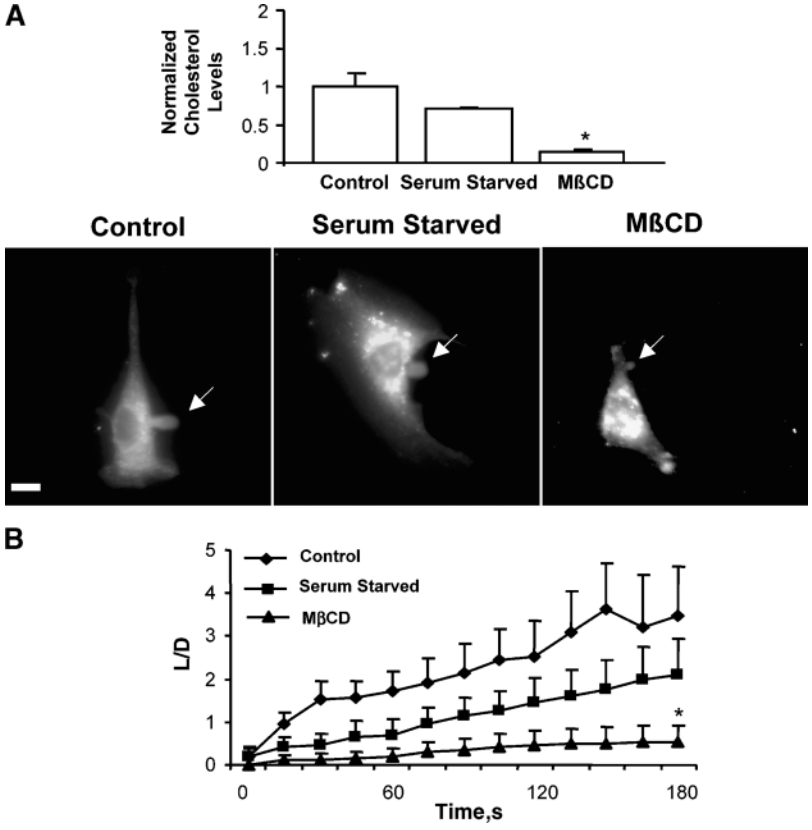

Fig. 5. Chronic and acute cholesterol depletion results in membrane stiffening of HAECs. Top: Free cholesterol in serum-starved and MβCD-treated HAECs. * $P < 0.05$. A: Typical images of membrane deformation of control, serum-starved, and MβCD-treated cells (−5 mm Hg). Arrows indicate the positions of the aspirated projections. Bar = 30 μm. B: Average time course of aspirated lengths for the three experimental cell populations at −5 mm Hg. The graphs show means + SEM. Control, n = 12; serum-starved, n = 4; MβCD-treated, n = 7.

follows: *1*) exposing HAECs to OxLDL results in strong cell stiffening; *2*) significant stiffening is also observed in PAECs freshly isolated from hypercholesterolemic pigs; and *3*) endothelial stiffening is accompanied by an increase in force generation and the ability of cells to form endothelial networks. We also show that all of the effects of OxLDL described above can be simulated by cholesterol depletion. We suggest, therefore, that OxLDL disrupts the integrity of endothelial lipid rafts, which in turn affects endothelial biomechanical properties and network formation. This is the first study to investigate the impact of OxLDL on endothelial biomechanics and its relationship to the formation of endothelial networks.

Multiple studies have demonstrated the presence of OxLDL in plasma and atherosclerotic lesions (3, 4, 31). In this study, low-passage HAECs, the best available cell model of human aortic endothelium, were exposed to a level of OxLDL similar to that in human plasma. Our data show that a short exposure to OxLDL was sufficient to cause significant endothelial stiffening, and a similar effect was observed in hypercholesterolemic pigs before the development of atherosclerotic lesions. Together, our in vitro and ex vivo data suggest that endothelial stiffening occurs in the early stage of atherosclerosis in vivo.

What are the possible mechanisms underlying the OxLDL-induced increases in endothelial stiffness and force generation? First, we considered the possibility that OxLDL may cause these effects by inducing cholesterol depletion. This hypothesis was based on two premises: *1*) earlier studies have shown that exposing endothelial cells to OxLDL or to oxidized phospholipids results in cholesterol depletion, particularly reducing the level of cholesterol in caveolae/lipid raft fractions (9, 32); and *2*) our observations that both the stiffening and the force generation effects are induced by depleting cellular cholesterol with MβCD. However, exploring this hypothesis by measuring cholesterol levels in different membrane fractions in OxLDL-treated cells, we have shown that exposure to OxLDL has no effect on cholesterol levels, either in low-density or high-density membrane fractions. Instead, we observed that both OxLDL exposure and MβCD-induced cholesterol depletion result in a decreased surface expression of GM_1, suggesting that lipid rafts were internalized, as described previously. Interestingly, ECs covering fatty streaks in vessels of cholesterol-fed rabbits have fewer caveolae, an effect that was simulated by cholesterol depletion in cultured ECs (33). We suggest, therefore, that the similarity between the effects of OxLDL and MβCD on HAEC biomechanics may be attributable to the redistribution of cellular cholesterol and the internalization of lipid rafts, which are known to modulate the coupling between the plasma membrane and the submembrane cytoskeleton (34–36). More specifically, we suggest that the stiffening effects may be related to the redistribution of a regulatory phospholipid, phosphatidylinositol bis phosphate, as was demonstrated for the cholesterol depletion-induced decrease in the lateral mobility of membrane proteins in fibroblasts (34). More studies are needed to test these hypotheses.

An increase in EC force generation was shown to facilitate the propensity of endothelial cells to form endothelial networks (20). Because neovascularization occurring

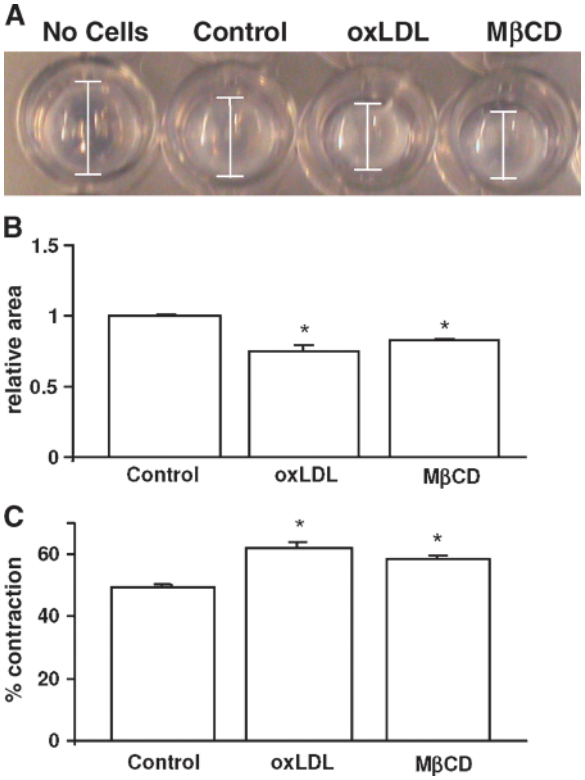

Fig. 6. Effect of OxLDL and MβCD on traction forces generated by HAECs. A: Typical images of collagen gel contraction by HAECs for control, cholesterol-depleted, and OxLDL-treated cells compared with gels containing no cells. Bars illustrate changes in gel size as a result of contraction by cells. B: Analysis of collagen gel contraction estimated as the area of the gels at 48 h after treatment normalized to controls. C: Percentage contraction of the gels for each experiment compared with gels without cells. The graphs show means + SEM. * $P < 0.05$.

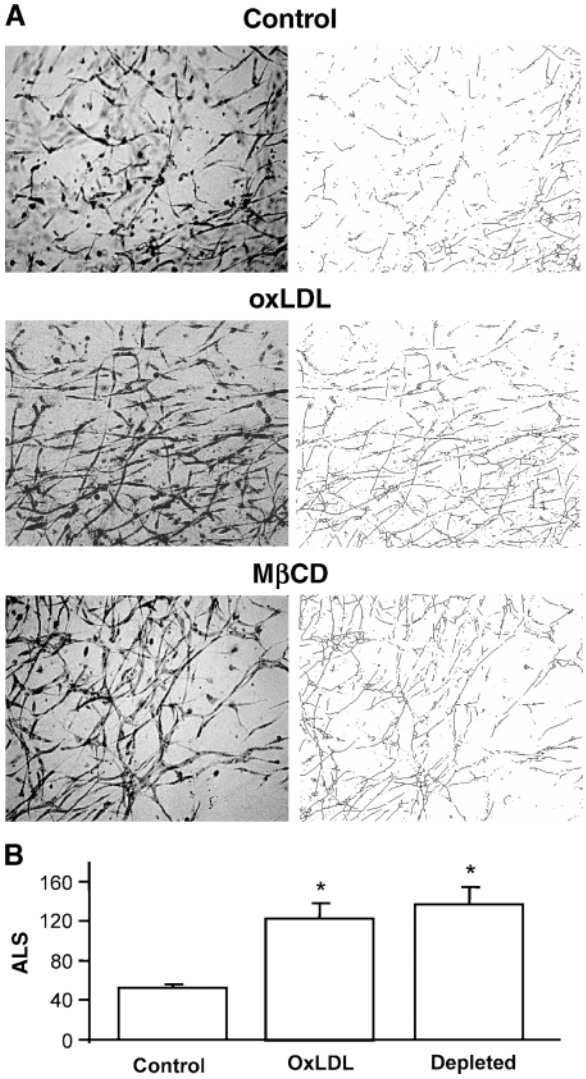

Fig. 7. OxLDL and MβCD facilitate elongation/connectivity of HAECs. A: Left, Images of HAECs network for control, depleted and OxLDL treated cell populations grown within collagen gels for 48 h. Right, skeletonized version of the images shown on the left. B: Quantification of network formation depicted in (A), as estimated by the average length of skeletonization (ALS). Same results were obtained in five separate experiments.

in atheromatous lesions is one of the major complications of atherosclerosis (37–39), it is important to determine how OxLDL-induced changes in EC biomechanics affect the potential for network formation. Several earlier studies have investigated the impact of OxLDL on different aspects of angiogenesis, such as endothelial cell proliferation (40–44), motility (10, 45, 46), and morphogenesis (11), but the findings are controversial. Specifically, although some studies have shown that OxLDL induces endothelial cell proliferation (42–44) and an increase in cell size (44), other studies have shown that OxLDL inhibits endothelial cell proliferation (40, 41) or even induces apoptosis (47, 48). It has been suggested that these discrepancies may be attributable to differences in OxLDL levels and exposure times and/or to interplay with other factors. In terms of cell motility and endothelial cell migration, the effect of OxLDL was shown to be inhibitory in an in vitro "scratched wound assay" (10, 45, 46), but there is still no sufficient information available about the effects of OxLDL on endothelial migration in three-dimensional cultures. Our study examines the effect of OxLDL on endothelial elongation (morphogenesis) and the formation of endothelial networks within a three-dimensional gel. Specifically, we show that although the number of lumens, which are formed from single cells (49, 50), is unaffected by OxLDL or MβCD, elongation of the cells is strongly facilitated.

On the surface, these observations are not consistent with the conclusion of an earlier study by Wang, Yang, and Chen (11), which reported that exposure to OxLDL resulted in a dose-dependent inhibition of endothelial cells isolated from human umbilical vein. However, the inhibitory concentrations of OxLDL used in that study (>200 μg/ml cholesterol) were much greater than those of the present study or in vivo. Specifically, the levels of OxLDL found in human plasma range between 7 and 35 μg/ml protein, which would correspond to ~15–75 μg/ml total cholesterol [an LDL particle contains

~47% cholesterol (9% and 38% unesterified cholesterol and cholesteryl ester respectively), ~11% triglyceride, ~22% phospholipid, and ~21% protein (51)]. It is noteworthy that, although not commented on by the authors (11), the lowest concentration of OxLDL tested increased the elongation of endothelial cells in another study, as we report here. Importantly, because an increase in endothelial elongation is generally believed to be one of the prerequisites of capillary network formation, we suggest that an OxLDL-induced increase in endothelial stiffness and force generation may facilitate neovascularization of the lesions. These observations support the concept that it is the interplay between the soluble and the mechanical signals and cell-matrix interactions that play the key role in the regulation of angiogenesis (52). It is also important to note that endothelial morphogenesis is only one of the important steps of capillary formation, and further studies are needed to investigate the role of cellular biomechanics in the regulation of endothelial proliferation and migration under different cholesterol conditions.

The authors thank Dr. Alisha Sieminski for helping with the analysis of EC networks. The authors also thank Mr. Yun Fang for helping with the isolation of pig endothelium, Dr. Michael Boretti and Mr. Jason Nichols for their help with gel histology, and Mr. Gregory Kowalsky for formatting figures performing F-actin staining of the gels and helping with cholera toxin experiments. The authors are grateful to Drs. Emile Mohler and Robert Wilensky for sharing aortic tissues of hypercholesterolemic and healthy pigs. This work was supported by a National Institutes of Health minority supplement (to F.J.B.), by American Heart Association Scientist Development Grant 0130254N (to I.L.), and by National Institutes of Health Grants HL-073965 and HD-045664 (to I.L.), HL-64388 (to Peter Francis Davies), and HL-22633 and HL-63768 (to G.H.R.).

REFERENCES

1. Berliner, J. A., and J. W. Heinecke. 1996. The role of oxidized lipoproteins in atherogenesis. *Free Radic. Biol. Med.* **20:** 707–727.
2. Steinberg, D. 2002. Atherogenesis in perspective: hypercholesterolemia and inflammation as partners in crime. *Nat. Med.* **8:** 1211–1217.
3. Yla-Herttuala, S., W. Palinski, M. E. Rosenfeld, S. Parthasarathy, T. E. Carew, S. Butler, J. L. Witztum, and D. Steinberg. 1989. Evidence for the presence of oxidatively modified low density lipoprotein in atherosclerotic lesions of rabbit and man. *J. Clin. Invest.* **84:** 1086–1095.
4. Holvoet, P., G. Theilmeier, B. Shivalkar, W. Flameng, and D. Collen. 1998. LDL hypercholesterolemia is associated with accumulation of oxidized LDL, atherosclerotic plaque growth, and compensatory vessel enlargement in coronary arteries of miniature pigs. *Arterioscler. Thromb. Vasc. Biol.* **18:** 415–422.
5. Hodis, H. N., D. M. Kramsch, P. Avogaro, G. Bittolo-Bon, G. Cazzolato, J. Hwang, H. Peterson, and A. Sevanian. 1994. Biochemical and cytotoxic characteristics of an in vivo circulating oxidized low density lipoprotein (LDL−). *J. Lipid Res.* **35:** 669–677.
6. Cazzolato, G., P. Avogaro, and G. Bittolo-Bon. 1991. Characterization of a more electronegatively charged LDL subfraction by ion exchange HPLC. *Free Radic. Biol. Med.* **11:** 247–253.
7. van Tits, L. J., T. M. van Himbergen, H. L. Lemmers, J. de Graaf, and A. F. Stalenhoef. Proportion of oxidized LDL relative to plasma apolipoprotein B does not change during statin therapy in patients with heterozygous familial hypercholesterolemia. *Atherosclerosis.* Epub ahead of print. July 7, 2005; doi:10.1016/j.atherosclersis.2005.06.006.
8. Gardner, G., C. L. Banka, K. A. Roberts, A. E. Mullick, and J. C. Rutledge. 1999. Modified LDL-mediated increases in endothelial layer permeability are attenuated with 17β-estradiol. *Arterioscler. Thromb. Vasc. Biol.* **19:** 854–861.
9. Blair, A., P. W. Shaul, I. S. Yuhanna, P. A. Conrad, and E. J. Smart. 1999. Oxidized low density lipoprotein displaces endothelial nitric-oxide synthase (eNOS) from plasmalemmal caveolae and impairs eNOS activation. *J. Biol. Chem.* **274:** 32512–32519.
10. Murugesan, G., and P. L. Fox. 1996. Role of lysophosphatidylcholine in the inhibition of endothelial cell motility by oxidized low density lipoprotein. *J. Clin. Invest.* **97:** 2736–2744.
11. Wang, D. Y., V. C. Yang, and J. K. Chen. 1997. Oxidized LDL inhibits vascular endothelial cell morphogenesis in culture. *In Vitro Cell. Dev. Biol. Anim.* **33:** 248–255.
12. Zeng, Y., N. Tao, K-N. Chung, J. E. Heuser, and D. M. Lublin. 2003. Endocytosis of oxidized low density lipoprotein through scavenger receptor CD36 utilizes a lipid raft pathway that does not require caveolin-1. *J. Biol. Chem.* **278:** 45931–45936.
13. Evans, E., and D. Needham. 1987. Physical properties of surfactant bilayer membranes: thermal transition, elasticity, rigidity, cohesion and colloidal interactions. *J. Phys. Chem.* **91:** 4219–4228.
14. Byfield, F., H. Aranda-Aspinoza, V. G. Romanenko, G. H. Rothblat, and I. Levitan. 2003. Cholesterol depletion constraints mechanical deformation of aortic endothelial cells (In IASTED International Conference on Biomechanics, Rhodos, Greece, June 30–July 2, 2003). ACTA Press.
15. Byfield, F., H. Aranda-Aspinoza, V. G. Romanenko, G. H. Rothblat, and I. Levitan. 2004. Cholesterol depletion increases membrane stiffness of aortic endothelial cells. *Biophys. J.* **87:** 3336–3343.
16. Pourati, J., A. Maniotis, D. Spiegel, J. L. Schaffer, J. P. Butler, J. J. Fredberg, D. E. Ingber, D. Stamenovic, and N. Wang. 1998. Is cytoskeletal tension a major determinant of cell deformability in adherent endothelial cells? *Am. J. Physiol. Cell Physiol.* **274:** C1283–C1289.
17. Sato, M., D. P. Theret, L. T. Wheeler, N. Ohshima, and R. M. Nerem. 1990. Application of the micropipette technique to the measurement of cultured porcine aortic endothelial cell viscoelastic properties. *J. Biomech. Eng.* **112:** 263–268.
18. Wang, N., I. M. Tolic-Norrelykke, J. Chen, S. M. Mijailovich, J. P. Butler, J. J. Fredberg, and D. Stamenovic. 2002. Cell prestress. I. Stiffness and prestress are closely associated in adherent contractile cells. *Am. J. Physiol. Cell Physiol.* **282:** C606–C616.
19. Barocas, V. H., and R. T. Tranquillo. 1997. An anisotropic biphasic theory of tissue-equivalent mechanics: the interplay among cell traction, fibrillar network deformation, fibril alignment, and cell contact guidance. *J. Biomech. Eng.* **119:** 137–145.
20. Sieminski, A. L., R. P. Hebbel, and K. J. Gooch. 2004. The relative magnitudes of endothelial force generation and matrix stiffness modulate capillary morphogenesis in vitro. *Exp. Cell Res.* **297:** 574–584.
21. Sieminski, A. L., R. P. Hebbel, and K. J. Gooch. 2005. Improved microvascular network in vitro by human blood outgrowth endothelial cells relative to vessel-derived endothelial cells. *Tissue Eng.* **11:** 1332–1345.
22. Park, H. J., D. Kong, L. Iruela-Arispe, U. Begley, D. Tang, and J. B. Galper. 2002. 3-Hydroxy-3-methylglutaryl coenzyme A reductase inhibitors interfere with angiogenesis by inhibiting the geranylgeranylation of RhoA. *Circ. Res.* **91:** 143–150.
23. Yang, S., J. Graham, W. K. Jeanne, E. A. Schwartz, and M. E. Gerritsen. 1999. Functional roles for PECAM-1 (CD31) and VE-cadherin (CD144) in tube assembly and lumen formation in three-dimensional collagen gels. *Am. J. Pathol.* **155:** 887–895.
24. Fang, Y., G. Schram, V. Romanenko, C. Shi, L. Conti, C. A. Vandenberg, P. F. Davies, S. Nattel, and I. Levitan. 2005. Functional expression of Kir2.x in human aortic endothelial cells: the dominant role of Kir2.2. *Am. J. Physiol. Cell Physiol.* **289:** C1134–C1144.
25. Passerini, A. G., D. C. Polacek, C. Shi, N. M. Francesco, E. Manduchi, G. R. Grant, W. F. Pritchard, S. Powell, G. Y. Chang, C. J. J. Stoeckert, et al. 2004. Coexisting proinflammatory and antioxidative endothelial transcription profiles in a disturbed flow region of the adult porcine aorta. *Proc. Natl. Acad. Sci. USA.* **101:** 2482–2487.
26. Blank, N. 2002. A fast, simple and sensitive method for the detection and quantification of detergent-resistant membranes. *J. Immunol. Methods.* **271:** 25–35.

27. Holvoet, P., A. Mertens, P. Verhamme, K. Bogaerts, G. Beyens, R. Verhaeghe, D. Collen, E. Muls, and F. Van de Werf. 2001. Circulating oxidized LDL is a useful marker for identifying patients with coronary artery disease. *Arterioscler. Thromb. Vasc. Biol.* **21:** 844–848.
28. Kincer, J. F., A. Uittenbogaard, J. Dressman, T. M. Guerin, M. Febbraio, L. Guo, and E. J. Smart. 2002. Hypercholesterolemia promotes a CD36-dependent and endothelial nitric-oxide synthase-mediated vascular dysfunction. *J. Biol. Chem.* **277:** 23525–23533.
29. Parton, R. G. 1994. Ultrastructural localization of gangliosides: Gm1 is concentrated in caveolae. *J. Histochem. Cytochem.* **42:** 155–166.
30. del Pozo, M. A., N. B. Alderson, W. B. Kiosses, H. H. Chiang, R. G. Anderson, and M. A. Schwartz. 2004. Integrins regulate rac targeting by internalization of membrane domains. *Science.* **303:** 839–842.
31. Weinbrenner, T., M. Cladellas, M. I. Covas, M. Fito, M. Tomas, M. Senti, J. Bruguera, and J. Marrugat. 2003. High oxidative stress in patients with stable coronary heart disease. *Atherosclerosis.* **168:** 99–106.
32. Yeh, M., A. L. Cole, J. Choi, Y. Liu, D. Tulchinsky, J-H. Qiao, M. C. Fishbein, A. N. Dooley, T. Hovnanian, K. Mouilleseaux, et al. 2004. Role for sterol regulatory element-binding protein in activation of endothelial cells by phospholipid oxidation products. *Circ. Res.* **95:** 780–788.
33. Darblade, B., D. Caillaud, M. Poirot, M. Fouque, J. C. Thiers, J. Rami, F. Bayard, and J. F. Arnal. 2001. Alteration of plasmalemmal caveolae mimics endothelial dysfunction observed in atheromatous rabbit aorta. *Cardiovasc. Res.* **50:** 566–576.
34. Kwik, J., S. Boyle, D. Fooksman, L. Margolis, M. P. Sheetz, and M. Edidin. 2003. Membrane cholesterol, lateral mobility, and the phosphatidylinositol 4,5-biphosphate-dependent organization of cell actin. *Proc. Natl. Acad. Sci. USA.* **100:** 13964–13969.
35. Nebl, T., K. N. Pestonjamasp, J. D. Leszyk, J. L. Crowley, S. W. Oh, and E. J. Luna. 2002. Proteomic analysis of a detergent-resistant membrane skeleton from neutrophil plasma membranes. *J. Biol. Chem.* **277:** 43399–43409.
36. Stahlhut, M., and B. van Deurs. 2000. Identification of filamin as a novel ligand for caveolin-1: evidence for the organization of caveolin-1-associated membrane domains by the actin cytoskeleton. *Mol. Biol. Cell.* **11:** 325–337.
37. Barger, A. C., R. Beeuwkes, L. L. Lainey, and K. J. Silverman. 1984. Hypothesis. Vasa vasorum and neovascularization of human coronary arteries. *N. Engl. J. Med.* **310:** 175–177.
38. Chen, F., P. Eriksson, T. Kimura, I. Herzfeld, and G. Valen. 2005. Apoptosis and angiogenesis are induced in the unstable coronary atherosclerotic plaque. *Coron. Artery Dis.* **16:** 191–197.
39. Virmani, R., F. D. Kolodgie, A. P. Burke, A. V. Finn, H. K. Gold, T. N. Tulenko, S. P. Wrenn, and J. Narula. 2005. Atherosclerotic plaque progression and vulnerability to rupture: angiogenesis as a source of intraplaque hemorrhage. *Arterioscler. Thromb. Vasc. Biol.* **25:** 2054–2061.
40. Chen, C-H., J. Cartwright, Jr., Z. Li, S. Lou, H. H. Nguyen, A. M. Gotto, Jr., and P. D. Henry. 1997. Inhibitory effects of hypercholesterolemia and ox-LDL on angiogenesis-like endothelial growth in rabbit aortic explants: essential role of basic fibroblast growth factor. *Arterioscler. Thromb. Vasc. Biol.* **17:** 1303–1312.
41. Chen, C-H., W. Jiang, D. P. Via, S. Luo, T-R. Li, Y-T. Lee, and P. D. Henry. 2000. Oxidized low-density lipoproteins inhibit endothelial cell proliferation by suppressing basic fibroblast growth factor expression. *Circulation.* **101:** 171–177.
42. Heinloth, A., K. Heermeier, U. Raff, C. Wanner, and J. A. N. Galle. 2000. Stimulation of NADPH oxidase by oxidized low-density lipoprotein induces proliferation of human vascular endothelial cells. *J. Am. Soc. Nephrol.* **11:** 1819–1825.
43. Kuhlmann, C. R., M. L. F. Schafer, T. Sawamura, H. Tillmanns, B. Waldecker, and J. Wiecha. 2003. Modulation of endothelial Ca(2+)-activated K(+) channels by oxidized LDL and its contribution to endothelial proliferation. *Cardiovasc. Res.* **60:** 626–634.
44. Seibold, S., D. Schurle, A. Heinloth, G. Wolf, M. Wagner, and J. Galle. 2004. Oxidized LDL induces proliferation and hypertrophy in human umbilical vein endothelial cells via regulation of p27kip1 expression: role of RhoA. *J. Am. Soc. Nephrol.* **15:** 3026–3034.
45. Chavakis, E., E. Dernbach, C. Hermann, U. F. Mondorf, A. M. Zeiher, and S. Dimmeler. 2001. Oxidized LDL inhibits vascular endothelial growth factor-induced endothelial cell migration by an inhibitory effect on the Akt/endothelial nitric oxide synthase pathway. *Circulation.* **103:** 2102–2107.
46. Murugesan, G., G. M. Chisolm, and P. L. Fox. 1993. Oxidized low density lipoprotein inhibits the migration of aortic endothelial cells in vitro. *J. Cell Biol.* **120:** 1011–1019.
47. Dimmeler, S., J. Haendeler, J. Galle, and A. M. Zeiher. 1997. Oxidized low-density lipoprotein induces apoptosis of human endothelial cells by activation of cpp32-like proteases: a mechanistic clue to the 'response to injury' hypothesis. *Circulation.* **95:** 1760–1763.
48. Galle, J., R. Schneider, A. Heinloth, C. Wanner, P. R. Galle, E. Conzelmann, S. Dimmeler, and K. Heermeier. 1999. Lp(a) and LDL induce apoptosis in human endothelial cells and in rabbit aorta: role of oxidative stress. *Kidney Int.* **55:** 1450–1461.
49. Bayless, K. J., and G. E. Davis. 2002. The cdc42 and rac1 GTPases are required for capillary lumen formation in three-dimensional extracellular matrices. *J. Cell Sci.* **115:** 1123–1136.
50. Davis, G. E., and K. J. Bayless. 2003. An integrin and rho GTPase-dependent pinocytic vacuole mechanism controls capillary lumen formation in collagen and fibrin matrices. *Microcirculation.* **10:** 27–44.
51. Chapman, J. M. 1986. Comparative analysis of mammalian plasma lipoproteins. *Methods Enzymol.* **128:** 70–143.
52. Ingber, D. E. 2002. Mechanical signaling and the cellular response to extracellular matrix in angiogenesis and cardiovascular physiology. *Circ. Res.* **91:** 877–887.